

## Modeling framework and associated simulation tools for the prediction of damage tolerance of CMC

Emmanuel Baranger<sup>a</sup>

LMT-Cachan (ENS Cachan/CNRS UMR8535/Université Paris Saclay), 61 av. du Président Wilson, 94235 Cachan Cedex, France

**Abstract.** A modeling framework and the associated simulation tools are presented for the prediction of the mechanical behaviour and lifetime of CMC with self-healing matrix. A macroscopic anisotropic damage model enriched with micro information has been developed, identified and validated using experimental information at different levels including reaction kinetics, fiber failure probability or macroscopic mechanical behavior. The computational cost associated to the proposed model being quite expensive, a method has been setup to construct, automatically, reduced numerical constitutive laws. An illustration is given as well as the associated error estimation.

With high manufacturing costs and moderated lifetimes at high temperatures, the use of CMC has been limited to military engine application. Nevertheless, recent developments on self-healing matrices have greatly increase their properties for long lifetimes. It is now possible to use them on civil engine applications in order to improve engine temperatures [1].

A first family of models have been developed to predict the mechanical behaviour of CMC under static loadings at the macroscopic scale [2–4]. For low lifetimes up to 5 000 h, a purely experimental approach allowed, for a high cost, to handle the problem of certification in the military domain. For civil application (expected lifetimes greater than 50 000 h) within the framework of damage tolerance, a direct experimental strategy becomes unaffordable. It becomes necessary to use models in order to anticipate the long term behavior over the whole loading range. A second family of models has been developed at LMT-Cacha [5–7]. The aim of these models is to predict the mechanical behavior but also the lifetime of the material. Loading cases accounted for in the model are static or cyclic mechanical loadings as well as thermal and chemical loadings (oxygen and steam pressures). To get robust results under multi-axial and multiphysic loadings, the model should rely on solid foundations. The aim of this paper is to present that kind of model and then how to implement and use them efficiently in a structural computation framework. First of all, note that a large amount of experimental information and models are available at different scales and on different mechanisms for this material [8–10]: from lifetimes on fibers to mechanical behavior on composite coupons by oxidation kinetics.

---

<sup>a</sup> e-mail: [baranger@lmt.ens-cachan.fr](mailto:baranger@lmt.ens-cachan.fr)

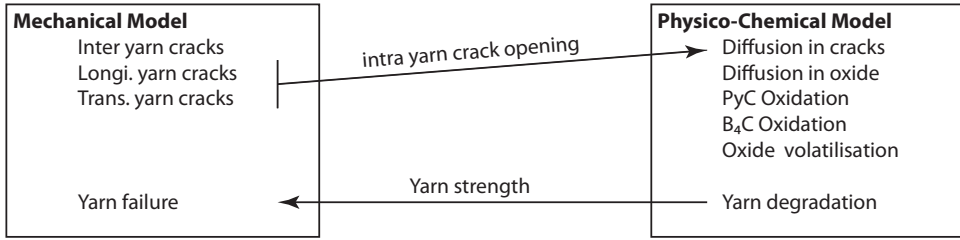


Figure 1. Modeling framework.

## 1. General modeling framework

The model follows the physics of the material. During a mechanical loading, the studied material (SiC/SiC with PyC interphase and self-healing matrix as in [11]) undergoes a complex cracking pattern. When this cracking pattern penetrates the yarns, oxygen can reach the fibers. SiC fibers suffer from subcritical crack growth at elevated temperature. Some of them fail after a certain time of exposure leading to the failure of the coupon. Self-healing matrix layers interact with oxygen to produce an oxid plug that fills the cracks. This mechanism slow down the diffusion of oxygen and thus extends greatly the lifetime of the material. The proposed model [7] can be divided in two parts. The first one, the mechanical one, aims at describing the different crack networks and the fiber failure. The second one, the physico-chemical one, aims at describing oxydation, diffusion and fiber degradation under air. The links between these two parts are: the crack opening indicator and the yarn strength. Figure 1 presents a scheme of the modeling framework with the main keypoints.

### 1.1 Mechanical model

The intra yarn crack network being the way of oxygen to reach the fibers, it is necessary to separate the different crack network contributions. From a global point of view, the crack network may be initially oriented by the loading directions (unknown a priori) and the oriented by the fabric directions. At the PyC interphase, cracks are deviated to avoid brittle failure of yarns.

The proposed mechanical model follows the work of [12–15]. First the damage kinematic is not defined a priori but imposed by evolution laws to account for the first steps of matrix cracking. Second, crack opening and closure effects are accounted using a separated form of the free energy. This energy reads:

$$e_d = \frac{1}{2} (Tr[C\sigma^+\sigma^+] + Tr[C_0\sigma^-\sigma^-] + Tr[Z\sigma\sigma]). \quad (1)$$

$C$  et  $Z$  are damage variables (4th order tensor) and  $C_0$  the initial compliance tensor. The first part is only activated in tension, the second in compression and the third in both cases.  $\sigma^+$  (resp.  $\sigma^-$ ) is the positive part (resp. negative) of stresses in the sens of the damage  $C$  (resp.  $C_0$ ) as explained in the appendix of [16].

Each degradation mechanism is described using a dedicated damage variable. Therefor, inter-yarn cracks, cracks in longitudinal yarns, cracks in transverse yarns have their own damage descriptions that cumulates through the law:

$$\dot{C} = \dot{C}_m + \dot{C}_f^{longi.} + \dot{C}_f^{trans.} + \dot{C}_{fatigue}^{longi.} + \dot{C}_{fatigue}^{trans.} \quad (2)$$

The *fatigue* lowerscript is related to the effect of wear on PyC interphases between fibers and matrix. The evolution of the anelastic strain follows the same kind of cumulative law without the inter-yarn term because wear is associated to sliding at the fiber/matrix interphase [17]. This fatigue term modeling is

based on a dimensional analysis and takes the following form [18]:

$$\dot{C}_{fatigue}^{longi} = \Delta C_{f+m}^{longi}(1, 1) \frac{-\dot{\Phi}(N)}{\Phi(N)^2} \frac{\Delta\sigma(1, 1)}{\sigma_{max}(1, 1)} \begin{pmatrix} f & 0 & 0 \\ 0 & 0 & 0 \\ 0 & 0 & 0 \end{pmatrix} \quad (3)$$

using the following wear function that varies between 0 and 1:

$$\Phi(N) = \frac{\exp(-\gamma_0 N) + \beta_0}{1 + \beta_0}. \quad (4)$$

$N$  is the number of equivalent cycles.  $\beta_0$  drives the saturation of wear,  $\gamma_0$  drives the speed of evolution of wear. The same form is used to model the anelastic strain evolution during cyclic loadings.

## 1.2 Crack opening indicator

The crack opening indicator (intra-yarn transverse cracks) is a keypoint for the coupling between the mechanical and physico-chemical parts. It allows to pass from the macroscopic description of the mechanical behavior to the description of the geometry of a mean crack in which the self-healing is developed. This indicator relies on the model from [17, 19].

Considering a fiber embedded in a matrix layer and submitted to tension, a Weibull distribution is used to describe the strength of the matrix layer. The shear stress that can be transmitted at the PyC interphase is supposed to depend of the cumulative slip during fatigue loading. This model has been identified on data from [20] on minicomposite and simulated using a finite element analysis. Different loading conditions are then simulated and a response surface built. It is then possible to define the evolution of the crack opening depending on the macroscopic damage variables. The crack density reads:

$$d_{longi} = (a\tau + b) \left( \Delta C_f^{longi} + \Delta C_{fatigue}^{longi} \right). \quad (5)$$

$\tau$  is the shear stress transmitted at the interphase. The crack opening indicator in longitudinal yarns reads:

$$h_{longi} = \frac{K_1}{d_{longi}} (\Delta C_f^{longi} + \Delta C_{fatigue}^{longi}) \sigma + \frac{K_2}{d_{longi}} \varepsilon_{ine}. \quad (6)$$

$K_1$  and  $K_2$  are coefficients representing the scale transition and are therefor identified at the macroscopic scale on the lifetime on coupons. However, we do not allow to get out of physical bound values for the crack opening indicators.

## 1.3 Physico-chemical model

### 1.3.1 Healing model

The physico-chemical model is based on the understanding of the underlying mechanisms presented in [21]. The objective of this part is to model the evolution of the yarn strength under oxidizing atmosphere. The main assumption is that self-healing is associated to the diffusion of oxygen in intra-yarn transverse cracks. The proposed model describes a mean crack as sketched on Fig. 2. The associated wireframe model is used to solve the diffusion/reaction/flow equations.  $F$  is the PyC oxidation front,  $D$  the maximum oxygen concentration near the fiber,  $E$  the healing layer oxidation front,  $C$  the plug limit and  $A$  is the oxygen entry point and also the volatilisation point in presence of steam. This simple structural model allows to account for many different situations such as healing, plug recession for various thermal and chemical loading conditions. From a history of crack opening indicator, the oxygen concentration history seen by the fibers can be computed.

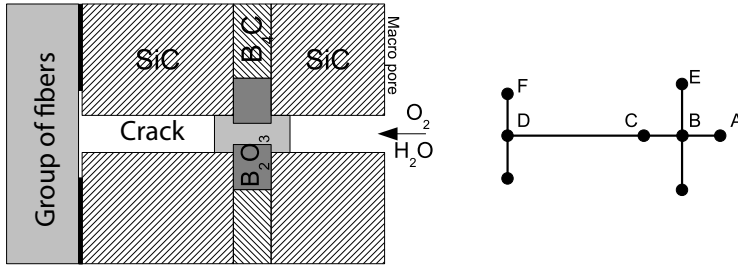


Figure 2. Healing sketch and associated wireframe resolution model.

### 1.3.2 Subcritical crack growth model

When oxygen reaches the fibers, their lifetime decreases without measurable damage. As shown in [22], only a small amount of fiber failures is necessary to get the failure of the yarn and thus their influence on the mechanical behavior at the scale of the composite is negligible. Available data from [8] on mono-filaments and yarns give the evolution of the lifetime of the fibers for a given constant loading (applied stress, temperature, oxygen pressure). For that, a model is proposed. It describes the evolution of the strength of the yarns  $\sigma_r$  to a cumulative oxygen concentration weighted by the temperature  $\Theta$ . This cumulative quantity is necessary to account for self-healing phases leading to varying oxygen concentration near the fibers. This law reads:

$$\Theta \sigma_r^n = B \tag{7}$$

with the cumulative oxygen concentration:

$$\Theta = \int_{time} C_{O_2} \exp\left(-\frac{E_a}{RT}\right) dt \tag{8}$$

where  $C_{O_2}$  is the oxygen concentration near the fibers computed by the wireframe model and T the imposed temperature.

## 2. Identification, validation

### 2.1 Identification

Concerning the macroscopic mechanical model, tension tests on coupons are used in axis and off axis. The global damage observed is attributed to the different contributions of the different crack networks based on the understanding of the development of the different crack networks.

Concerning the fatigue modeling, cyclic fatigue tests have been conducted on coupons in [23] and are directly used for identification of the macromodeling of fatigue.

Concerning the reaction/diffusion model, the experimental data from [10, 24] are used for the reaction kinetics, diffusion and volatilization constants. The morphology is directly taken from micrographs, the sequential layers deposition being controlled and leading to a clear morphology definition. Concerning the crack opening indicator, only the form is kept and one parameter needs to be determined at the macroscale:  $(K_1, K_2)$  of equation 6. For that, a static fatigue test is used. This test gives the lifetime of a composite for a constant 200 MPa longitudinal loading at 500°C in air [25].

The identification is performed at three scales, micro, meso and macroscopic:

- microparameters: multi-layered matrix morphology, chemistry, sub-critical crack growth of fibers/yarns;
- mesoparameters: fiber volume content;

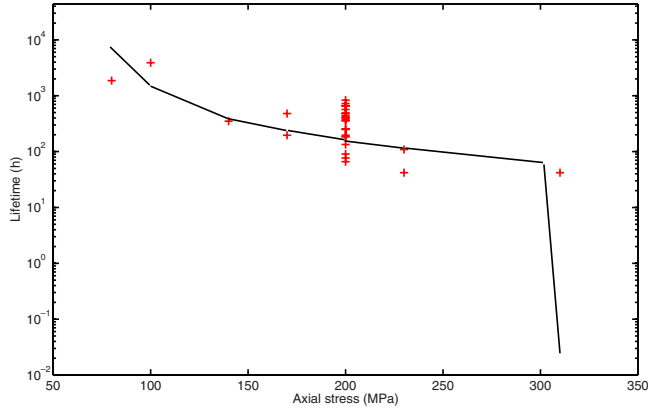


**Figure 3.** Lifetime versus applied stress for a temperature of 500°C, 20 kPa oxygen partial pressure and 1,8 kPa water vapor partial pressure. + experimental data, – model prediction.

- macroparameters: mechanical behavior for static and fatigue loadings based on static tests. The crack opening magnification ( $K$ ) uses the mean lifetime value for a test under axial stress of 200 MPa, with a temperature of 500°C, 20 kPa of oxygen partial pressure and 1.8 kPa water vapor partial pressure. The corresponding mean lifetime of 250 h can be seen via the set of tests in the middle of Fig. 3.

## 2.2 Validation

Further identification of the lifetime modeling for static fatigue loading is realized on coupons at 200 MPa and for a temperature of 500°C. The influence of the stress and temperature is presented in the whole model via the damage mechanisms (and corresponding crack networks), via the oxidizing of the matrix, via the oxide volatilization and via the subcritical cracking of the fibers. It is thus interesting to compare the model response with different case of loading (applied stress and temperature levels) for which experimental results are available (mainly in tension). From an experimental point of view, the test corresponding to the highest lifetime corresponds to five months and a half (4000 h) for an applied stress of 100 MPa. The experimental lifetimes are quite short because too complex to control beyond few months while the expected lifetimes for industrial applications is about five years (4.4 10<sup>4</sup> h). For the sake of simplicity, the first comparison relates to the influence of the applied stress. The experiment/simulation comparison is presented Fig. 3 and shows the influence of the tension loading level for a constant temperature of 500°C and oxygen and water vapor partial pressures of 200 kPa and 1.8 kPa.

On the range of the experimental results, the model is in good agreement considering the mean slope as well as the highest variation for low stress levels. On the other hand, for applied stresses close to the static limit, the model predicts a sharp decline of the strength before the initial strength level.

## 3. Mechanical model reduction

The macroscopic mechanical model proposed has been implemented in Abaqus to treat first structural cases related to damage tolerance. Open hole plates computations are presented in [26] as well as the implementation. The definition of the positive and negative parts in Eq. (1) implies the eigenvalue decomposition of the compliance and stress tensors and thus leads to an expansive computational cost. This cost can be legitimate for high level of loadings but not for low levels leading to long

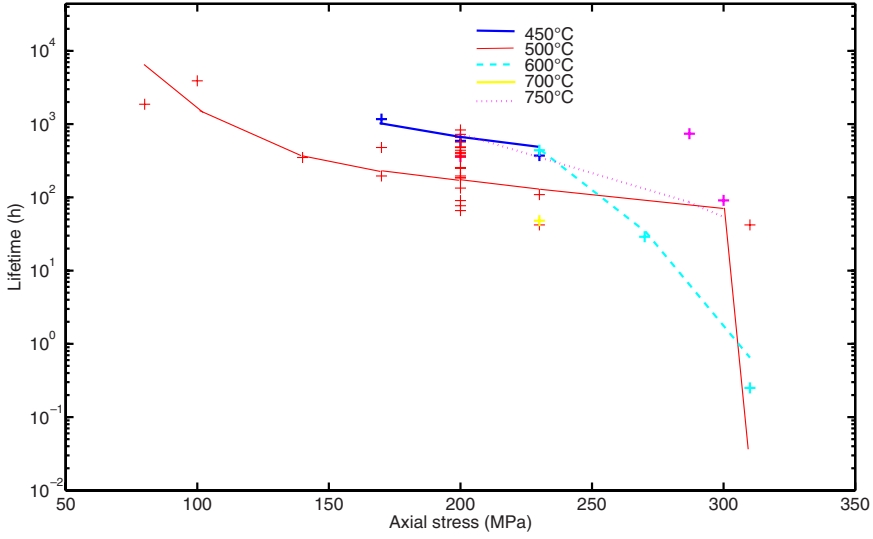


**Figure 4.** Lifetime versus applied stress for different temperatures.

lifetimes on civil applications. In this part, an approach for the automatic building of a cheaper model is given [16, 27].

A Singular Value Decomposition (SVD) is used to find the best decomposition basis to represent the field of damage variables for a given set of representative states corresponding to a representative set of loading conditions.

In a first approach, a numerical potential approximation is avoided by assuming the following form of the strain energy density to represent Eq. (1):

$$\tilde{e}_d(\sigma, d_i) = \frac{1}{2} Tr \left[ \left( C_0 + \sum_i d_i C_i \right) \sigma \sigma \right] \quad (9)$$

where  $(d_i)_i$  is the new, reduced, set of damage variables. This potential still uses  $\sigma$  as state variable and is quite simple. In this approach, the form of the chosen potential is crucial because:

- it defines the meaning of the internal variables;
- it must be adapted to the complexity of the constitutive law to describe. If not adapted, the resulting reduced law may be inaccurate.

Note that, due to the simple form of the approximate potential, continuous damage evolution laws are sufficient to get continuous stress/strain relations.

Thus the SVD will try to determine the best damage kinematic  $C_i$  (these modes form an orthogonal basis) in a certain range of loadings, minimizing the error:

$$e^2 = \sum_{states} Tr [C_{err} C_{err}]. \quad (10)$$

This considers the sum of the errors on the load range (states) accounted for the reduced model evaluation. The sum is therefore performed for all time steps for the different considered loading paths i.e. for each considered state of loading.

$$C_{err} = (C_0 + d_i C_i) - \frac{\partial^2 e_d}{\partial \sigma^2} |_{damage}. \quad (11)$$

**Table 1.** Percentage explained for each mode of the PCA.

| Mode        | 1       | 2      | 3      | 4      | 5      | 6      |
|-------------|---------|--------|--------|--------|--------|--------|
| % explained | 94.7041 | 2.6930 | 2.3848 | 0.1991 | 0.0187 | 0.0002 |

**Table 2.** Modes of the PCA.

|                        |                    |        |         |         |         |         |         |
|------------------------|--------------------|--------|---------|---------|---------|---------|---------|
| $\hat{C}_{11}$         | $C_{1111}$         | 0.1191 | -0.6987 | 0.5923  | -0.3674 | 0.1090  | -0.0014 |
| $\hat{C}_{22}$         | $C_{2222}$         | 0.1191 | 0.6987  | 0.5923  | -0.3674 | -0.1090 | -0.0014 |
| $\hat{C}_{33}$         | $C_{1212}$         | 0.9776 | -0.0000 | -0.2093 | -0.0204 | 0.0000  | -0.0042 |
| $\sqrt{2}\hat{C}_{12}$ | $\sqrt{2}C_{1122}$ | 0.0161 | -0.0000 | 0.0474  | 0.0777  | 0.0000  | 0.9957  |
| $\sqrt{2}\hat{C}_{13}$ | $2C_{1112}$        | 0.0883 | 0.1090  | 0.3552  | 0.6015  | 0.6987  | -0.0653 |
| $\sqrt{2}\hat{C}_{23}$ | $2C_{2212}$        | 0.0883 | -0.1090 | 0.3552  | 0.6015  | -0.6987 | -0.0653 |

This error compares the approximation of the compliance  $C_0 + d_i C_i$  and the compliance of the original model. The term  $\frac{\partial^2 e_d}{\partial \sigma^2} |_{damage}$  is the secant compliance also noted  $\frac{\partial e^e}{\partial \sigma}$ .

The SVD is performed on  $\frac{\partial e^e}{\partial \sigma} - C_0$  that is some kind of damage compliance. The minimization classically reads:

$$\min_{span(C_i)} e^2 = \min_{span(C_i)} \left( \sum_{loads} Tr [C_{err} C_{err}] \right) \quad (12)$$

$$= \max_{span(C_i)} \left( \sum_{loads} \sum_i d_i d_i \right) \quad (13)$$

$$= \max_{span(C_i)} \left( \sum_i \sum_{loads} \left( Tr \left[ \left( \frac{\partial e^e}{\partial \sigma} - C_0 \right) C_i \right] \right)^2 \right) \quad (14)$$

$$= \max_{span(C_i)} \sum_i \frac{Tr \left[ C_i \left( \sum_{loads} \left( \frac{\partial e^e}{\partial \sigma} - C_0 \right) \otimes \left( \frac{\partial e^e}{\partial \sigma} - C_0 \right) \right) C_i \right]}{Tr [C_i C_i]} \quad (15)$$

The error is minimal for  $C_i$  maximizing the Rayleigh quotient:

$$R(U) = \frac{Tr \left[ U \left( \sum_{loads} \left( \frac{\partial e^e}{\partial \sigma} - C_0 \right) \otimes \left( \frac{\partial e^e}{\partial \sigma} - C_0 \right) \right) U \right]}{Tr [UU]} \quad (16)$$

The set  $(C_i)_i$  is then obtained by solving the associated eigen-value problem.  $C_i$  having the major and minor symmetries, this problem can be solved using matrix libraries and two successive Voigt notations.  $(C_i)_i$  are the eigenvectors and  $(\alpha_i)_i$  the associated eigenvalues. This methodology has been applied to proportional loading paths up to 150 MPa.

Six modes can be computed (in the Voigt notation), the percentage explained for each mode is presented in Table 1. The chosen Voigt notation is the same for stress and strain  $(\sigma_{11}, \sigma_{22}, \sqrt{2}\sigma_{12})$ . The percentage explained of the mode i is given by:  $\frac{\alpha_j}{\sum_j \alpha_j}$ .

In Table 2 are presented the modes of the PCA. The first one corresponds to the description of the shear while the second and third correspond to the description of the on-axis tractions.

The relative error on the potential can be computed for a truncated expansion, it is presented in Table 3. Based on this table, one or two modes should be sufficient. Nevertheless, as the evolution law

**Table 3.** Relative error on the potential.

| Truncation order | 1  | 2   | 3   | 4    | 5    | 6 |
|------------------|----|-----|-----|------|------|---|
| % Error (%)      | 10 | 4.5 | 1.8 | 0.32 | 6E-3 | 0 |

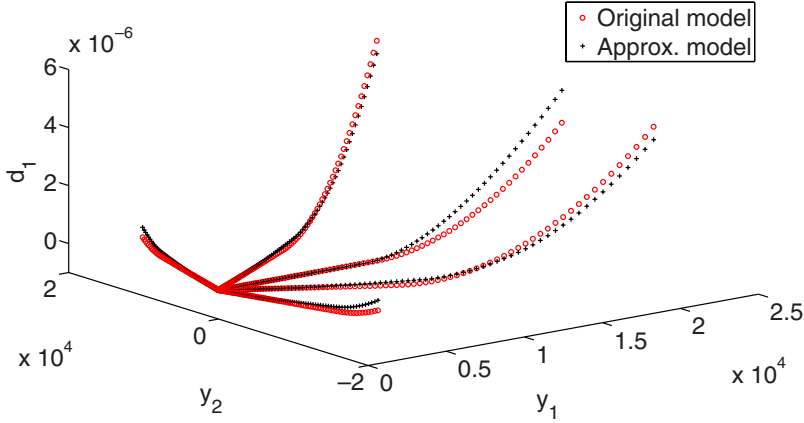


**Figure 5.** Evolution law for  $d_1$ .

will be also approximated, the error will be greater. In practice, only the two first modes are retained for the illustration.

The thermodynamical force associated to the new damage variable  $d_i$  is:

$$y_i = \frac{\partial \tilde{e}_d}{\partial d_i} = \frac{1}{2} Tr[C_i \sigma \sigma]. \tag{17}$$

Thus, introducing the thermodynamical forces associated to  $C$  and  $Z$  (named  $Y$  and  $Y'$ ), the computation of  $y_i$  is quite easy in Voigt notation:

$$y_i = Tr[C_i Y]. \tag{18}$$

On Fig. 5 is presented the evolution of the damage variables  $d_1$  versus the associated thermodynamical forces  $y_1$  and  $y_2$  for the considered range of loading. On that basis, approximated evolution laws have been identified and plotted on the same figure. Another way, more accurate but less efficient regarding the computational cost, is to build a response surface for each damage variable. The same kind of figure can be plotted for  $d_2$ .

Note that if the kinematic of the model is not rich enough then the evolution laws may become quite complicated. The computational cost is greatly decreased using the reduced constitutive relation. For example, for 505 runs covering the whole loading path set, the average cost ratio is:

$$\frac{COST_{original}}{COST_{reduced}} = 1500. \tag{19}$$

#### 4. Conclusion et perspectives

A macroscopic model has been proposed to predict the mechanical behavior as well as the lifetime of self-healing ceramic matrix composites. Each physical mechanism is modeled independently and coupled with other mechanisms using small structural models in order to have robust prediction in case of complex loadings thus enriching the basic macroscopic model. It allows taking into account

experimental data from different scales on different physics from cracking to oxidation. The proposed model has been validated on a wide range of mechanical and thermal loadings, mainly for constant applied conditions. Such a model, even macroscopic, is useful to better understand the scenario of degradation/healing of the material. It has been implemented in a structural context. To decrease an expansive computational cost, a model reduction technique is proposed to automatically build a cheaper model accurate for a reduced loading range.

This model can still be enriched including probabilistic features. First attempts can be found in [28, 29]. This model also has to be used and compared to real structural cases.

The author acknowledges the members of the projects *CPR Modélisation, extrapolation, validation de la durée de vie des CMC, FUI ARCOCE, RAPID PRESID* as well as SAFRAN Herakles and DGA for their financial support.

## References

- [1] M. Bourgeon, *Thermostructural materials in aerospace industry: applications and standardization*, in *Proceedings of the 7th International Conference on High Temperature Ceramic Matrix Composites* (Bayreuth (Germany), 2010)
- [2] X. Aubard, J. Lamon, O. Allix, *Journal of the American Ceramic Society* **77**, 2118 (1994)
- [3] L. Guillaumat, J. Lamon, *Composites Science and Technology* **56**, 803 (1996)
- [4] A. Gasser, P. Ladeveze, M. Poss, *Composites science and technology* **56**, 779 (1996)
- [5] S. Letombe, C. Cluzel, P. Ladevèze, *A macroscopic model coupling oxidation and damage for CMCs*, in *Proceedings of JNC13 conference* (2003), pp. 713–722
- [6] S. Letombe, Ph.D. thesis, ENS-Cachan (2005)
- [7] C. Cluzel, E. Baranger, P. Ladevèze, A. Mouret, *Composites Part A: Applied Science and Manufacturing* **40**, 976 (2009)
- [8] W. Gauthier, J. Lamon, R. Pailler, *Revue des Composites et Matériaux Avancés* **16**, 221 (2006)
- [9] M. Moevus, N. Godin, M. R'Mili, D. Rouby, P. Reynaud, G. Fantozzi, G. Farizy, *Composites Science and Technology* **68**, 1258 (2008), cited By (since 1996): 14
- [10] F. Rebillat, X. Martin, A. Guette, *proceedings of HTCMC* **5**, 321 (2004)
- [11] F. Lamouroux, S. Bertrand, R. Pailler, R. Naslain, M. Cataldi, *Composites science and technology* **59**, 1073 (1999)
- [12] P. Ladeveze, *Proc. CNRS Int. Coll* **351**, 355 (1983)
- [13] A. Gasser, P. Ladevèze, P. Pérès, *Materials Science and Engineering A* **250**, 249 (1998)
- [14] P. Ladevèze, S. Letombe, C. Cluzel, *A CMC Damage Model Based on Micro-and Macromechanics for High-Temperature and Complex Loading*, in *High Temperature Ceramic Matrix Composites* (Wiley Online Library, 2001), pp. 578–583
- [15] P. Ladevèze, *An anisotropic damage theory with unilateral effects: applications to laminates and to three-and four-dimensional composites*, O. Allix and F. Hild edn. (Elsevier, 2002)
- [16] E. Baranger, *International Journal of Damage Mechanics* **22**, 1222 (2013)
- [17] D. Rouby, P. Reynaud, *Composites Science and Technology* **48**, 109 (1993)
- [18] P. Ladevèze, E. Baranger, M. Genet, C. Cluzel, *Ceramic Matrix Composites: Materials, Modeling and Technology* (John Wiley & Sons, Inc., 2014), chap. Damage and Lifetime Modeling for Structure Computations, pp. 465–519, n. P. Bansal and J. Lamon eds, ISBN: 978-1-118-23116-6, 712 pages
- [19] P. Reynaud, *Composites Science and Technology* **56**, 809 (1996)
- [20] N. Lissart, J. Lamon, *Journal of materials science* **32**, 6107 (1997)
- [21] P. Forio, J. Lamon, *Ceramic Transactions(USA)* **128**, 127 (2001)
- [22] O. Loseille, J. Lamon, **112**, 129 (2010)

- [23] O. Penas, P. Reynaud, D. Rouby, G. Fantozzi, *Self-Healing SiCf/SiC Composite Behaviour under High-Temperature Cyclic Fatigue in Air*, in *High Temperature Ceramic Matrix Composites* (Wiley Online Library, 2001), pp. 480–485
- [24] F. Rebillat, E. Garitte, A. Guette, Design, Development, and Applications of Engineering Ceramics and Composites pp. 135–149 (2010)
- [25] M. Moevus, M., Ph.D. thesis, INSA-Lyon (2007)
- [26] M. Genet, L. Marcin, E. Baranger, C. Cluzel, P. Ladevèze, A. Mouret, *Composites Part A: Applied Science and Manufacturing* **43**, 294 (2012)
- [27] O. Friderikos, E. Baranger et al., *Dimensionality reduction of a complex constitutive law for Ceramic Matrix Composites*, in *2nd ECCOMAS Young Investigators Conference (YIC 2013)* (2013)
- [28] E. Baranger, *Modeling Of The Evolution Of The Failure Probability Of A Self-Healing Ceramic Matrix Composite*, in *ECCM 15–15th European Conference on Composite Materials* (Venice (Italy), 2012)
- [29] E. Baranger, J. Lamon, *Modelling of stochastic features in damage and life of a self-healing ceramic matrix composite in air at high temperatures*, in *DURACOSYS 2014–11th International Conference on Durability Analysis of Composite Systems* (Tokyo, 2014)